Organic & Biomolecular Chemistry

ROYAL SOCIETY OF CHEMISTRY

PAPER

View Article Online
View Journal | View Issue

Cite this: *Org. Biomol. Chem.*, 2022, **20**, 387

Four- and two-armed hetero porphyrin dimers: their specific recognition and self-sorting behaviours†

Masahiro Ueda,[a] Masaki Kimura,[a] Shinobu Miyagawa,[a] Masaya Naito,[a] Hikaru Takaya[b,c] and Yuji Tokunaga*[a]

In this study we self-assembled the four-armed porphyrin hetero dimer capsule **Cap4**, stabilized through amidinium–carboxylate salt bridges, in CH_2Cl_2 and $CHCl_3$. The dimer capsule **Cap4** was kinetically and thermodynamically more stable than the corresponding two-armed dimer **Cap2**. The number of arms strongly influenced their recognition behaviour; guests possessing small aromatic faces (*e.g.*, 1,3,5-trinitrobenzene) preferred residing in the cavity of the two-armed capsule **Cap2**, rather than in **Cap4**, both thermodynamically and kinetically; in contrast, large aromatic guests (*e.g.*, 9,10-dibromoanthracene) were encapsulated predominantly by **Cap4** because of favourable entropic effects. The number of arms enabled self-sorting behaviour of the dimer formation; complexation studies using an equimolar mixture of the four porphyrin constituents of the two capsules revealed the quantitative formation of the corresponding dimers **Cap2** and **Cap4**. Furthermore, we examined the specific molecular recognition of **Cap2** and **Cap4**; NMR experiments of mixtures of **Cap2** and **Cap4** in the presence of favourable guests for **Cap2** and **Cap4** revealed that these guest molecules were encapsulated selectively by their preferred hosts.

Received 28th August 2021,
Accepted 25th November 2021

DOI: 10.1039/d1ob01694f

rsc.li/obc

Introduction

The porphyrins have often been used as significant units in supramolecular architectures.[1] In addition to the unique properties of porphyrins allowing them to be used as catalysts for chemical reactions[2] and to induce specific photophysical and/or electrochemical behaviour,[3,4] multiporphyrinic functional systems can also provide discrete spaces for molecular recognition and sensing.[5] For example, coordination-driven porphyrin cages have been developed to encapsulate biologically relevant molecules in their cavities.[6] Porphyrin cages also have been exploited as hosts for aromatic guest molecules, with stabilization occurring as a result of the large area of the aromatic porphyrin rings.[7] Co-facial dimeric porphyrin containers can incorporate flat aromatic guests with high association constants;[8] expanding the distance between the porphyrin units can allow porphyrin cages to accommodate three-dimensional aromatic guests (*e.g.*, fullerenes)[9] or several guest molecules in the form of multilayer π-aromatic structures.[9b,10]

Recently, we reported the construction of a hetero dimer **Cap2′** from a pair of two-armed porphyrin derivatives, **P1** and **P2a**, stabilized by complementary amidinium–carboxylate salt bridges in aprotic and nonpolar solvents (Fig. 1a and 2); this dimer host encapsulated electron-deficient aromatic compounds inside its cavity, forming heteromeric three-layer π-aromatic structures.[11] Furthermore, we have synthesized a D_2-symmetric trimeric porphyrin host complex, comprising the two- and four-armed porphyrins **P1** and **P4a**, that recognizes aromatic guests, forming highly organized π-aromatic structures.[12] To construct higher-order assembled multilayer π-aromatic architectures from porphyrin derivatives bearing complementary hydrogen-bonding pairs (*e.g.*, aminoquinolino and carboxy functionalities), we would need to introduce a "complementary number" of binding pairs. For example, Fig. 1c provides a cartoon representation of a 3 : 2 mixture of a four-armed hydrogen-bond-acceptor porphyrin **P4** and a six-armed hydrogen-bond-donor porphyrin **P5** that might selectively form a heteromeric porphyrin pentamer through the assembly of two four-armed and two two-armed complementary hydrogen bonding pairs. Such a porphyrin pentamer would possess four cavities positioned between porphyrin

[a]*Department of Materials Science and Engineering, Faculty of Engineering, University of Fukui, Bunkyo, Fukui 910-8507, Japan. E-mail: tokunaga@u-fukui.ac.jp*
[b]*International Research Centre for Elements Science, Institute for Chemical Research, Kyoto University, Uji 611-0011, Japan*
[c]*Institute for Molecular Science, National Institute of Natural Science, Nishigo-Naka, Myodaiji, Okazaki 444-8585, Japan*

† Electronic supplementary information (ESI) available: NMR and mass spectra, NMR titration data, and Arrhenius plots. See DOI: 10.1039/d1ob01694f

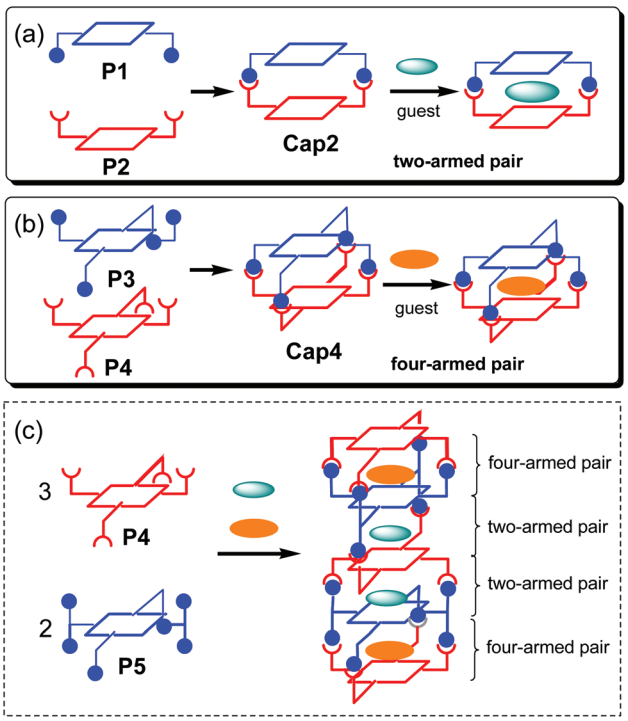

Fig. 1 Cartoon representation of hetero porphyrin oligomer capsules and their molecular recognition: (a) a two-armed porphyrin dimer **Cap2** formed from **P1** and **P2**, (b) a four-armed porphyrin dimer **Cap4** formed from **P3** and **P4**, and (c) a porphyrin pentamer formed from **P4** and **P5**.

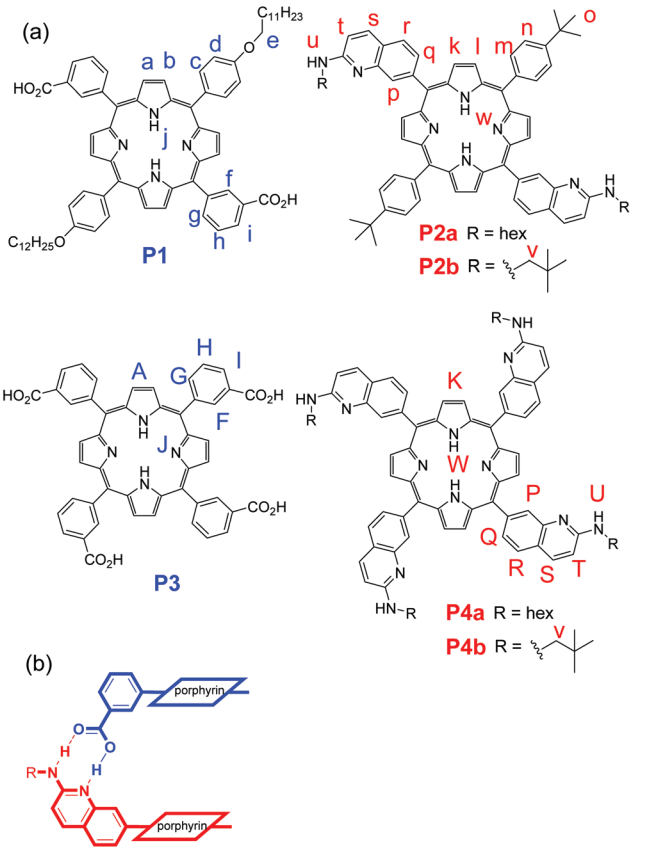

Fig. 2 (a) Structures of the porphyrin derivatives used to prepare the self-assembled dimers. (b) Cartoon representation of the amidinium–carboxylate salt bridge and the resulting parallel arrangement of the two porphyrin rings.

faces, two of each type (two- and four-armed), that could potentially bind different types of aromatic guests depending on their flexibility and rigidity. Prior to construction of such a porphyrin pentamer, we wished to confirm whether a "complementary number" of binding pairs would allow specific formation of porphyrin oligomers and, if so, investigate their molecular recognition properties.

In this paper we report the construction and molecular recognition behaviour of the hetero four-armed dimer capsule **Cap4** from the components **P3** and **P4b** (Fig. 1b), and compare it with the corresponding two-armed dimer **Cap2** (**Cap2′**) formed from components **P1** and **P2b** (**P2a**). In addition, we observed self-sorting behaviour of a mixture of **P1–P4** to form the two capsules **Cap2** and **Cap4** selectively. Herein, we also demonstrate the results of competitive molecular recognition experiments of the dimers in the presence of aromatic guests.

Results and discussion

Design and synthesis of porphyrin derivatives P2b and P4b

We examined formation of four-armed porphyrin dimer formed from porphyrin derivatives **P3** and **P4a**, which was previously synthesized,[12] first of all. Although the signals originated from the dimer **P3·P4a** appeared in the ^{1}H NMR spectrum of an equimolar mixture of **P3** and **P4a** in $CDCl_3$, the signals of other assembled species were observed in the spectrum.[13] Therefore, bulky neopentylamino group instead of hexylamino group in porphyrin derivatives **P2** and **P4** was chosen for this study to prevent the formation of other species. Scheme 1 presents the synthesis of neopentylaminoquinolino porphyrin derivatives **P2b** and **P4b**. Aminations of chloride **1**[11] with neopentylamine afforded aminoaldehyde **2**, after hydrolysis of imino group. Treatment of the aldehyde **2** with dipyrromethane **3**[11] and pyrrole in propionic acid gave two-armed and four-armed porphyrin derivatives **P2b** and **P4b**, respectively.

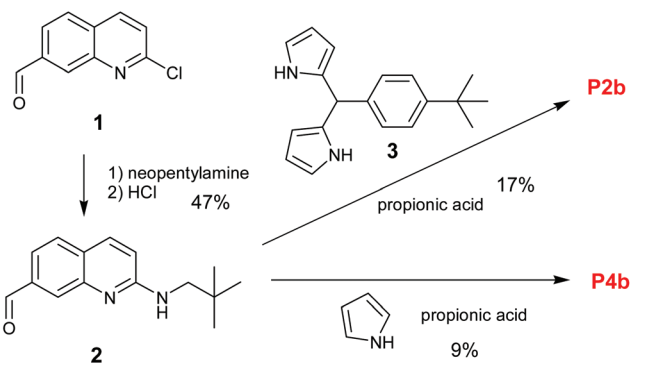

Scheme 1 Synthesis of the porphyrin derivatives **P2b** and **P4b**.

Formation of four-armed dimer Cap4

We used NMR spectroscopy to confirm the formation of the porphyrin dimer **Cap4**. The ^{1}H NMR spectrum (600 MHz, $CDCl_3$, 25 °C) of a 1 : 1 mixture of the porphyrin derivatives **P3** and **P4b** possessed no signals of the individual component; they had been replaced by a new single set of signals (Fig. 3 and S1†). The signal of the aminoquinoline NH_U units shifted downfield from 4.97 to 11.67 ppm, while the signals of the NH units at the centres of both porphyrins appeared at significantly high fields (moving from −2.65 and −2.82 ppm to −3.63 ppm for H_W and H_J), consistent with the formation of the four-armed dimer capsule **P3·P4b** (**Cap4**) with co-facial arrangement of its two porphyrin rings (Fig. 2b). These low- and high-field shifts were quite similar to those of the two-armed dimer **P1·P2a** (**Cap2′**). The mass spectrum (ESI) of a solution containing a 1 : 1 mixture of **P3** and **P4b** featured a peak at *m*/*z* 1949.8565 (calcd 1949.8609), corresponding to the four-armed dimer [**Cap4** + H]$^+$ (Fig. S4†).

Kinetic and thermodynamic stabilities of each porphyrin dimer in the presence of competitive solvent (DMSO)

In aprotic and nonpolar solvents, such as $CHCl_3$ and CH_2Cl_2, both dimers (**Cap2** and **Cap4**) formed quantitatively from equivalent mixtures. To weaken the hydrogen bonds between the aminoquinolino and carboxy groups, we prepared equimolar solutions of **P1** and **P2b** in mixtures of $CDCl_3$ and DMSO-d_6. In the ^{1}H NMR spectra of mixtures of **P1** and **P2b** in $CDCl_3$/DMSO-d_6 (from 100 : 0 to 65 : 35), the signals of the porphyrin NH units of the two-armed dimer **Cap2** appeared near −3.6 ppm and those of the corresponding monomers appeared in the range from −2.6 to −2.9 ppm (Fig. 4 and S5†); the signals of the dimer broadened in the 98 : 2 mixture, and only the signals for the monomers appeared in the 65 : 35 mixture of $CDCl_3$/DMSO-d_6. In corresponding solutions of the four-armed dimer (**Cap4**), small signals appeared in the ^{1}H NMR spectrum for the monomers when the content of DMSO-d_6 was 34%, whereas **Cap4** had dissociated completely when the content of DMSO-d_6 was 66% (Fig. 5 and S6†). Thus, the four-armed dimer **Cap4** was more stable than the two-armed **Cap2**.

Next, we evaluated the thermodynamic stabilities of both dimers. In the ^{1}H NMR spectrum [600 MHz, $CDCl_3$/DMSO-d_6 (80 : 20)] of an equimolar mixture of **P1** and **P2b** (0.50 mM) at −50 °C, the signals for the porphyrin NH units appeared at −3.80 ppm for **Cap2** and at −2.97 and −3.02 ppm for its monomers (Fig. 6 and S7†). Upon increasing the temperature, the ratio of **Cap2** decreased. From integration of these signals for **Cap2** and the monomers, we calculated the dimerization constant (K_d) to be 6700 (M^{-1}) at −20 °C. The Arrhenius plots of the data for the formation of **Cap2** yielded a straight line (Fig. S9a†), from which we calculated the thermodynamic para-

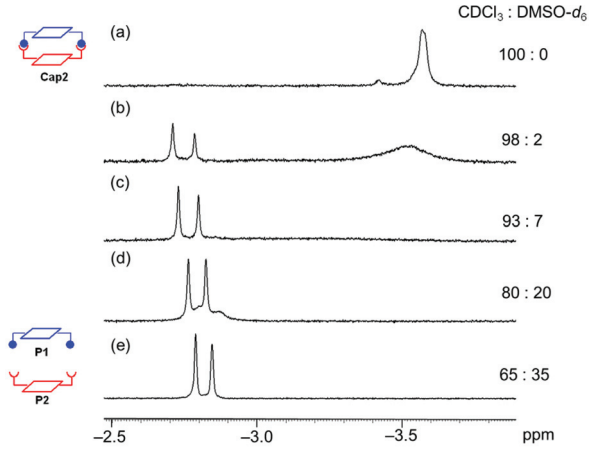

Fig. 4 Partial ^{1}H NMR spectra (600 MHz, 25 °C) of a 1 : 1 mixture (0.50 mM) of **P1** and **P2b** (a) in $CDCl_3$, (b) in $CDCl_3$/DMSO-d_6 (98 : 2), (c) in $CDCl_3$/DMSO-d_6 (93 : 7), (d) in $CDCl_3$/DMSO-d_6 (80 : 20), and (e) in $CDCl_3$/DMSO-d_6 (65 : 35).

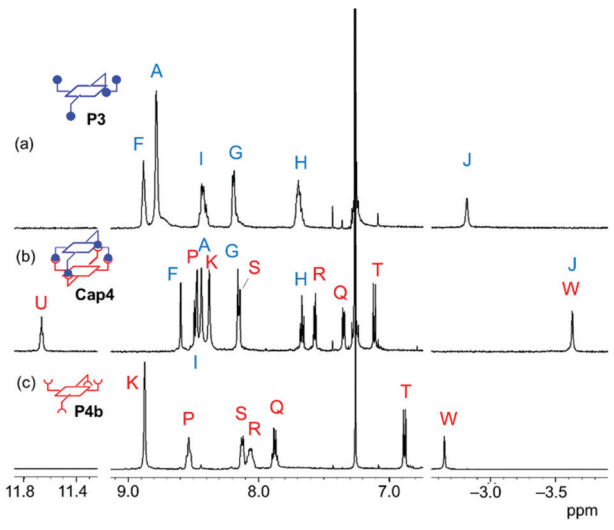

Fig. 3 Partial ^{1}H NMR spectra (600 MHz, $CDCl_3$) of (a) the porphyrin derivative **P3** in the presence of Et_3N (5.0 eq.), (b) a 1 : 1 mixture (0.50 mM) of the porphyrin derivatives **P3** and **P4b** (**Cap4**), and (c) the porphyrin derivative **P4b**.

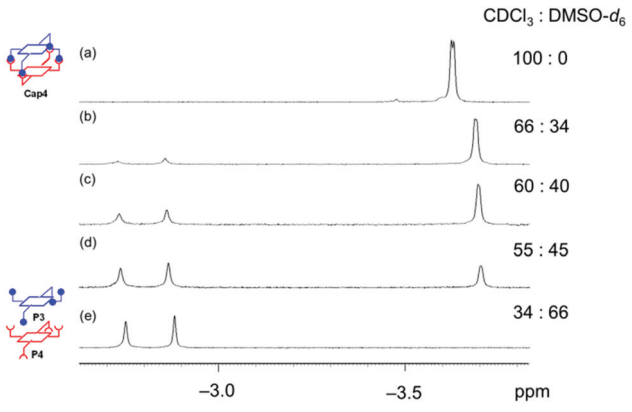

Fig. 5 Partial ^{1}H NMR spectra (600 MHz, 25 °C) of a 1 : 1 mixture (0.50 mM) of **P3** and **P4b** (a) in $CDCl_3$, (b) in $CDCl_3$/DMSO-d_6 (66 : 34), (c) in $CDCl_3$/DMSO-d_6 (60 : 40), (d) in $CDCl_3$/DMSO-d_6 (55 : 45), and (e) in $CDCl_3$/DMSO-d_6 (34 : 66).

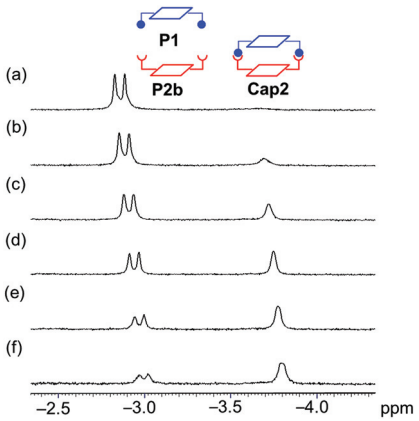

Fig. 6 Partial ^{1}H NMR spectra [600 MHz, $CDCl_3$/DMSO-d_6 (80 : 20), 0.50 mM] of a 1 : 1 mixture of **P1** and **P2b** at (a) 0 °C, (b) −10 °C, (c) −20 °C, (d) −30 °C, (e) −40 °C, and (f) −50 °C.

Table 1 Thermodynamic parameters of the formation of the hetero porphyrin dimers **Cap2** and **Cap4** [a]

Dimer	K_d [M^{-1}]	ΔH [kJ mol^{-1}]	ΔS [J K^{-1} mol^{-1}]	Solvent
Cap2[b]	6700 ± 260 (−20 °C)	−36 ± 0.76	−72 ± 2.2	$CDCl_3$/ DMSO-d_6 (80 : 20)
Cap4[c]	9200 ± 1400 (20 °C)	−54 ± 3.4	−109 ± 12	$CDCl_3$/ DMSO-d_6 (55 : 45)

[a] The thermodynamic parameters were obtained from the VT NMR experiments. The NMR experiments were performed more than twice, and the average is shown. [b] 0.50 mM solution of **P1** and **P2b** was examined from −50 to 0 °C. [c] 0.50 mM solution of **P3** and **P4b** was examined from 0 to 50 °C.

meters (Table 1). In a similar manner, variable temperature (VT) NMR spectra (600 MHz, from 0 to 50 °C, 0.50 mM) of an equimolar solution of **P3** and **P4b** in $CDCl_3$/DMSO-d_6 (55 : 45) (Fig. S8†) allowed us to estimate the thermodynamic parameters for the formation of **Cap4** (Fig. S9b† and Table 1).

The dimerization constant for the four-armed dimer **Cap4** was higher than that for the two-armed **Cap2**, even though the conditions for forming the two-armed dimer were more favourable than those of the four-armed dimer [two-armed: in $CDCl_3$/DMSO-d_6 (80 : 20) at −20 °C; four-armed: in $CDCl_3$/DMSO-d_6 (55 : 45) at 20 °C]. Thus, formation of the four-armed dimer **Cap4** was enthalpically favourable—the result of increasing the number of complementary hydrogen bonds. Nevertheless, the presence of four strong interactions was associated with the entropic cost of decreasing the flexibility of the rigid dimer structure.

Recognition of small aromatic guests by Cap2 and Cap4

We reported previously that the dimer **Cap2′** could accommodate the electron-deficient aromatic guests **G_1–G_5**, each featuring one or two rings, to form three-layer π-aromatic structures.[11] We used NMR spectroscopy to obtain the association constants for the interactions of the four-armed capsule **Cap4** with these same guest molecules (Fig. S10–S14†). Similar to the behaviour with **Cap2′**, the rates of association and dissociation of **Cap4** and its guests were fast on the NMR spectroscopic time scale at 25 °C; therefore, we used BindFit software[14] to calculate the association constants (K_a, Table 2) for encapsulation from the changes in chemical shifts. The association constants for the interactions of the two-armed dimer **Cap2′** with the guests **G1–G5** were 13–51 times larger than those of the four-armed dimer **Cap4**, even though they contained the same types of porphyrin units. We recorded VT NMR spectra of a mixture of **Cap4** and the guest **G1** to evaluate the rates of association and dissociation of complexation (Fig. S10d†). Individual signals appeared for **Cap4** and **G1@Cap4** when the temperature was less than −40 °C. In comparison, for the corresponding mixture of **Cap2′** and **G1**, the signals of the complexed and uncomplexed species were detected separately when the temperature was below −20 °C.[11] Thus, the complex **G1@Cap2′** was also kinetically more stable than that of **G1@Cap4**, even though the four arms of the latter

Table 2 Association constants (K_a, M^{-1}) for the interactions of aromatic guests with the hetero dimers **Cap2** and **Cap4** at 25 °C

		Solvent	K_{Cap2}/K_{Cap4}
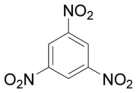 **G1**	**Cap2′**: K_a = 49 000 ± 4400[a,b] **Cap4**: K_a = 2190 ± 450[c]	CH_2Cl_2 CD_2Cl_2	22
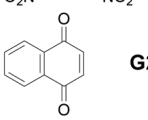 **G2**	**Cap2′**: K_a = 330 ± 32[a,b] **Cap4**: K_a = 18 ± 3.2[c]	CD_2Cl_2 CD_2Cl_2	18
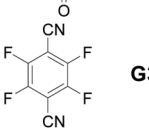 **G3**	**Cap2′**: K_a = 6700 ± 680[a,b] **Cap4**: K_a = 132 ± 27[c]	CD_2Cl_2 CD_2Cl_2	51
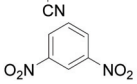 **G4**	**Cap2′**: K_a = 280 ± 16[a,b] **Cap4**: K_a = 18 ± 4.2[c]	CD_2Cl_2 CD_2Cl_2	16
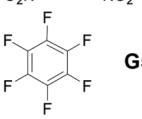 **G5**	**Cap2′**: K_a = 30 ± 2[a,b] **Cap4**: K_a < 2.4[c,d]	CD_2Cl_2 CD_2Cl_2	>13
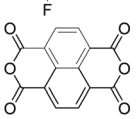 **G6**	**Cap2**: ND[e] **Cap4**: K_a > 10 000[f]	 $CDCl_3$/ DMSO-d_6 (93/7)	—
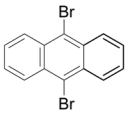 **G7**	**Cap2**: K_a = 80 ± 1.7[e] **Cap4**: K_a = 680 ± 77[f]	$CDCl_3$ $CDCl_3$	1/8

[a] Ref. 12. [b] **Cap2′** formed from **P1** and **P2a**. [c] Solutions of **Cap4** and guests were examined twice; BindFit software was used to calculate the association constants, and average values are shown. [d] A series of titration experiments did not give a valid value. [e] **Cap2** formed from **P1** and **P2b**. [f] Solutions of **Cap4** (0.50 mM) and guests were examined; association constants were calculated from integration of signals from each species.

could have better encapsulated the guest moiety in the complex. We suspect that stronger π-stacking interactions in the **G1@Cap2′** complex resulted in slower dissociation.

Recognition of large and rigid guest by Cap2 and Cap4

Next, we examined naphthalenetetracarboxylic anhydride (**G6**), possessing a larger aromatic surface, as a rigid guest for the dimeric hosts **Cap2** and **Cap4**. Because **G6** is insoluble in $CDCl_3$, we used a small amount of DMSO-d_6 as a co-solvent (Fig. S17†). In the ^{1}H NMR spectrum [600 MHz, $CDCl_3$/DMSO-d_6 (87 : 13)] of a mixture of **Cap2** (0.50 mM) and **G6** (1.5 mM), signals for the complex appeared independent of those averaged for **Cap2** and the monomers **P1** and **P2b**. For example, the signals of the pyrrole NH units of the complex **G6@Cap2** appeared at −5.79 and −5.66 ppm, while the averaged signals of **Cap2** and the monomeric species appeared at −2.94 ppm; this shifting is consistent with the shielding effects of the guest **G6**. In addition, the signal of naphthalene moiety in the complex **G6@Cap2** appeared at 4.53 ppm; the complex **G6@Cap2** was the major species in solution at 25 °C when 3.0 eq. (1.5 mM) of **G6** were present. We suspect that **G6** induced the assembly of the three components because it is a suitable guest for the porphyrin dimer. Because DMSO interfered with the formation of **Cap2**, as described above, we could not estimate the association constant for the interaction of **Cap2** and **G6** through integration of the signals of the various species; in addition, small unidentified signals appeared near −4.5 ppm.

In a similar manner, we performed titration experiments of **Cap4** and **G6** (Fig. S18†). The rates of association and dissociation and the formation of the capsule **Cap4** were slow on the NMR spectroscopic timescale. The ^{1}H NMR spectrum [600 MHz, $CDCl_3$/DMSO-d_6 (91 : 9)] of a mixture of **Cap4** (0.50 mM) and **G6** (1.0 mM) featured the signals of the pyrrole NH protons of **G6@Cap4** shifted significantly upfield (−5.90 and −5.64 ppm) and the signal of the complexed **G6** at 4.82 ppm. The ROESY spectrum featured a cross-peak for the complexed and uncomplexed signals of **G6** (4.82 and 8.82 ppm), based on association and dissociation. We tried to estimate an association constant for **G6@Cap4** [in $CDCl_3$/DMSO-d_6 (93 : 7), at 25 °C], however the signal for the free **G6** was too small to integrate accurately because of strong association (Fig. S18b†). We were able to assign all of the signals of the complexes **G6@Cap2** and **G6@Cap4** through two-dimensional (2D) NMR experiments (Fig. S19–S22†).

Next, was examined the behaviour of 9,10-dibromoanthracene (**G7**) as a guest for the dimers. Shifting of the signals of the protons of **Cap2** in its ^{1}H NMR spectrum (600 MHz, $CDCl_3$, 25 °C) occurred upon the addition of **G7** (0–3.45 mM) (Fig. 7 and S23a†). For example, the signals of the pyrrole NH protons of **Cap2** shifted significantly upfield (Fig. 7k: *ca.* −4.0 ppm in the presence of 6.9 eq. of **G7**), consistent with the shielding effects of the guest **G7**. From the signal shifting and the concentrations of the guest **G7**, we used BindFit software to estimate an association constant (K_a) of 80 (M^{-1}) at 25 °C.[14]

We performed titration experiments of **Cap4** and **G7** (Fig. 8 and S27†). In this case, the rates of association and dissociation for the complexation of **Cap4** and **G7** were slow on the NMR spectral timescale at room temperature, as similar to the case of **Cap4** and **G6**. For example, individual signals for the complexed and uncomplexed species are evident in the ^{1}H NMR spectrum (600 MHz, $CDCl_3$) of a mixture of **Cap4** and **G7**: signals of "uncomplexed" pyrrole NH protons appearing at −3.63 ppm and those of their "complexed" counterparts at −5.74 and −5.46 ppm. From integration of these corresponding species, we calculated an association constant of 680 M^{-1} (Table 2).

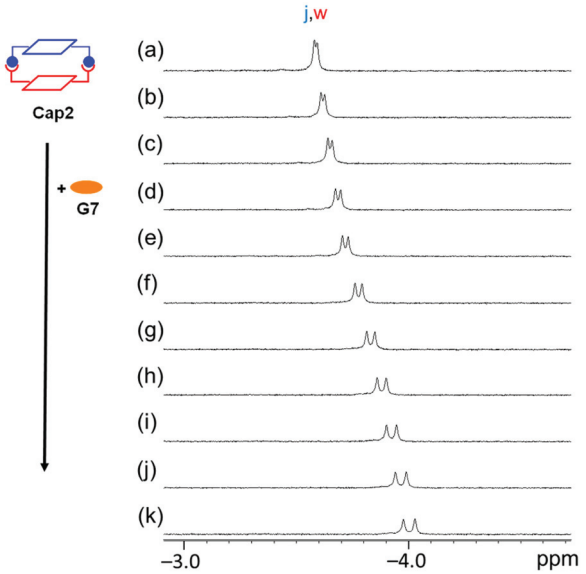

Fig. 7 Partial ^{1}H NMR spectra (600 MHz, $CDCl_3$, 20 °C) of a mixture of **Cap2** (0.5 mM) and **G7** (0–3.45 mM): (a) **Cap2**; (b) **Cap2** and **G7** (0.20 mM); (c) **Cap2** and **G7** (0.40 mM); (d) **Cap2** and **G7** (0.60 mM); (e) **Cap2** and **G7** (0.80 mM); (f) **Cap2** and **G7** (1.25 mM); (g) **Cap2** and **G7** (1.65 mM); (h) **Cap2** and **G7** (2.1 mM); (i) **Cap2** and **G7** (2.55 mM); (j) **Cap2** and **G7** (3.0 mM); and (k) **Cap2** and **G7** (3.45 mM).

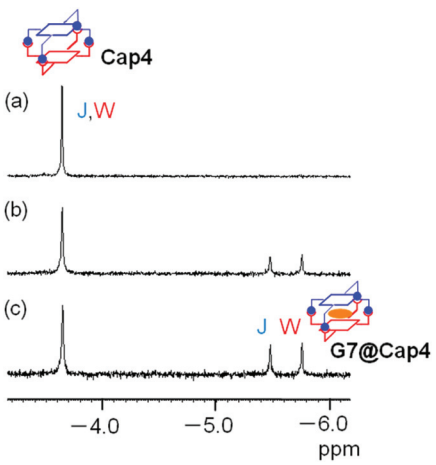

Fig. 8 Partial ^{1}H NMR spectra (600 MHz, $CDCl_3$, 25 °C) of mixtures of **Cap4** (0.50 mM) and **G7** (0–1.5 mM): (a) **Cap4**; (b) **Cap4** and **G7** (1.0 mM); (c) **Cap4** and **G7** (1.5 mM).

Interestingly, the association constant for the binding of **G7** in **Cap4** was approximately eight times greater than that in **Cap2**, while the rates of association and dissociation of **Cap4** were slower than those of **Cap2**. These kinetic and thermodynamic results are completely opposite from those obtained when using 1,3,5-trinitrobenzene (**G1**) as the guest.

Thermodynamic parameters for complexation of dimers and G7

We used VT NMR spectral titration to evaluate the thermodynamic details of the recognition behaviour of the dimer hosts **Cap2** and **Cap4** for complexation. Upon decreasing the temperature, the relative concentrations of the complexes **G7@Cap2** and **G7@Cap4** increased. From Arrhenius plots recorded using the association constants for the dimers (**Cap2** and **Cap4**) and **G7** from −20 to 50 °C and from −50 to 50 °C (Fig. S23–S28†), we estimated the various thermodynamic parameters of these systems, respectively (Table 3). The formation of both complexes was enthalpically favourable, but complexation of **G7@Cap2** was entropically disfavoured. We suspect that two porphyrin rings in the relatively flexible **Cap2** dimer underwent stacking with the anthracene ring to form the complex **G7@Cap2** with a resulting loss of freedom. In contrast, the more rigid **Cap4** dimer could accommodate **G7** without a large degree of conformational restriction.

As described above, the values of K_a for the interactions of **Cap2** with the small guests **G1–G5** were larger than those for the interactions of **Cap4** with the same guests; whereas rigid and large-area guests were recognized predominantly by **Cap4**, the large value for the entropy of **Cap4** contributed to this discrimination.

Competitive self-sorting of a mixture of the porphyrins P1–P4

Many self-assembled systems have been developed that display self-sorting, with specific structures formed rather than all of the possible noncovalent complexes of the compounds present.[15] The specific assembled structures that form, thermodynamically or kinetically, from all of the possible noncovalent complexes are controlled by the number of binding sites. For example, Lehn *et al.* observed the selective formation of homomeric double strands from a mixture of four oligobipyridines of different length;[16] this approach has also been applied to the specific formation of heteromeric aggregates stabilized by complementary hydrogen bonds.[17] In these cases, the substrate bearings different numbers of binding sites differed in terms of their molecular lengths. In the case of **Cap2** and **Cap4**, however, the number of arms is different, but the molecular sizes of these units are quite similar.

The partial ^{1}H NMR spectrum of an equimolar mixture of the porphyrin derivatives **P1–P4** (Fig. 9 and S29†) reveals signal for only the two dimers, **Cap2** and **Cap4**, as expected. Because **Cap4** was the more thermodynamically stable dimer, it formed predominantly in solution, with the remaining **P1** and **P2b** units thereafter forming the dimer **Cap2**.

Competitive encapsulation of Cap2 and Cap4

Next, we examined the specific molecular recognition of **Cap2** and **Cap4**; that is, we recorded NMR spectra of mixtures of **Cap2** and **Cap4** in the presence of favourable guests (**G1** and **G6**, respectively). First, we added 1,3,5-trinitrobenzene (**G1**) to a solution of **Cap2** (0.50 mM) and **Cap4** (0.50 mM) in $CDCl_3$ (Fig. 10 and S30†). The ^{1}H NMR spectrum of a mixture of **Cap2**, **Cap4**, and **G1** (0.25 mM) at −50 °C (Fig. 10b) featured the signal of H_u of **G1@Cap2** at 11.8 ppm. Upon increasing the concentration of **G1**, the signal of H_U of **G1@Cap4** appeared at 11.7 ppm at the same temperature. The signal of H_U of **G1@Cap4** was negligible initially, and **G1** was encapsulated when it was present more than 1.0 eq. (0.50 mM). When the spectra of the same samples were recorded at 25 °C (Fig. S30b†), the signals of **Cap2** shifted preferentially when

Table 3 Thermodynamic parameters of the formation of the complexes **G7@Cap2** and **G7@Cap4** in $CDCl_3$[a]

Dimer	K_a [M^{-1}][b]	ΔH [kJ mol^{-1}]	ΔS [J K^{-1} mol^{-1}]
Cap2[c]	80 ± 1.7	−15 ± 1.1	−15 ± 3.7
Cap4[d]	680 ± 77	−12 ± 0.01	15 ± 0.90

[a] The thermodynamic parameters were obtained from the VT NMR experiments. [b] At 25 °C. [c] Solutions of **Cap2** (0.50 mM) with **G7** (0–3.45 mM) were examined from 0 to 25 °C and from −20 to 50 °C, and BindFit software was used to calculate the association constants. Average values of the association constants and thermodynamic parameters are shown. [d] A solution of **Cap4** (0.50 mM) with **G7** (1.0 mM) was examined from −50 to 50 °C twice, the association constants were calculated from integrations of the corresponding species. Average values of the association constants and thermodynamic parameters are shown.

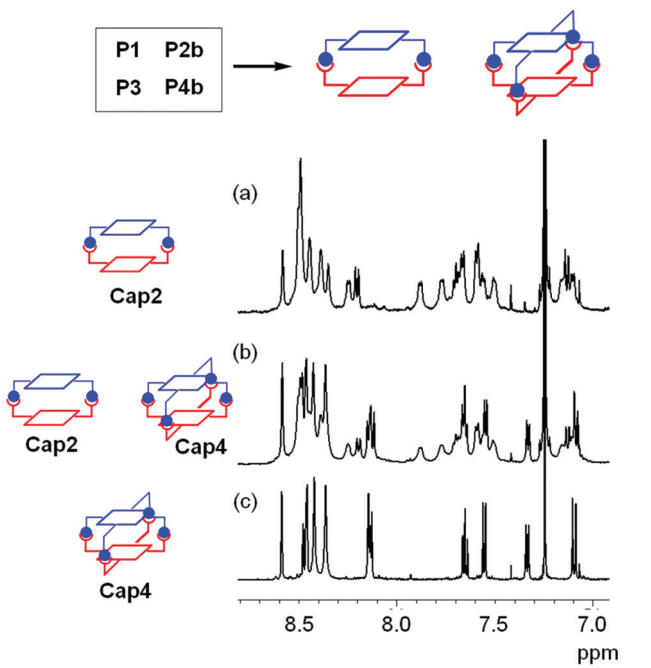

Fig. 9 Partial ^{1}H NMR spectra (600 MHz, $CDCl_3$, 25 °C) of equimolar (0.50 mM) mixtures of the porphyrin derivatives. (a) **P1** and **P2b** (**Cap2**); (b) **P1**, **P2b**, **P3**, and **P4b**; and (c) **P3** and **P4b** (**Cap4**).

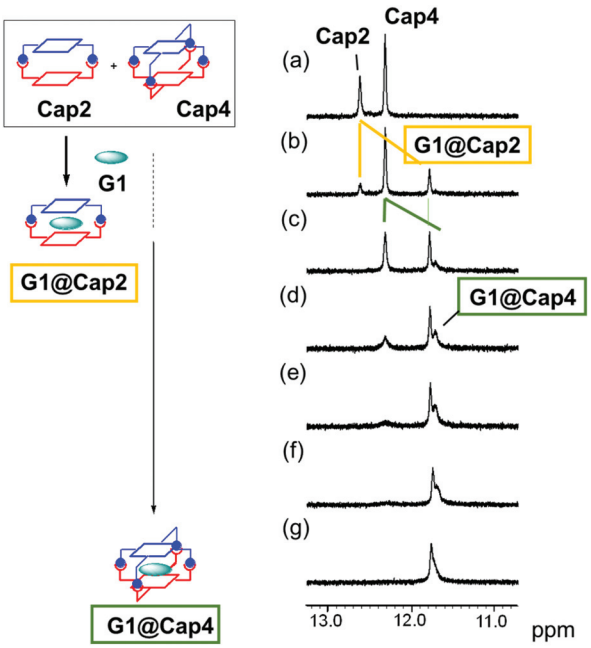

Fig. 10 Partial ^{1}H NMR spectra (600 MHz, $CDCl_3$, −50 °C) of mixtures of **Cap2** (0.50 mM), **Cap4** (0.50 mM), and **G1** (0–2.0 mM): (a) **Cap2** and **Cap4**; (b) **Cap2**, **Cap4**, and **G1** (0.25 mM); (c) **Cap2**, **Cap4**, and **G1** (0.50 mM); (d) **Cap2**, **Cap4**, and **G1** (0.75 mM); (e) **Cap2**, **Cap4**, and **G1** (1.0 mM); (f) **Cap2**, **Cap4**, and **G1** (1.25 mM); and (g) **Cap2**, **Cap4**, and **G1** (2.0 mM).

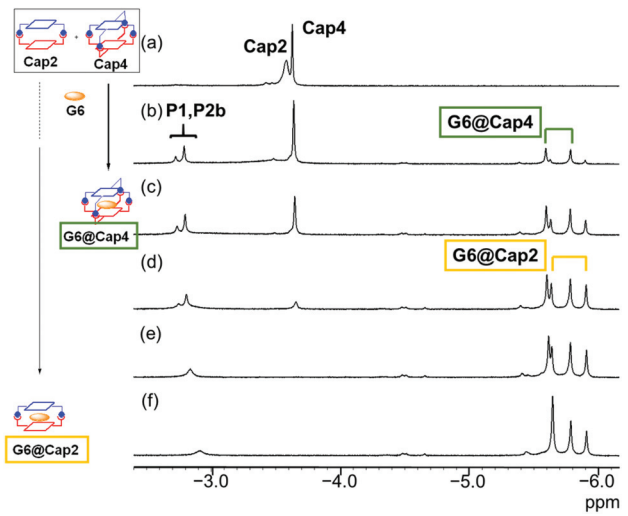

Fig. 11 Partial ^{1}H NMR spectra (600 MHz, 25 °C) of mixtures of **Cap2** (0.50 mM) and **Cap4** (0.50 mM) in the presence of **G6** (0–1.25 mM): (a) **Cap2** and **Cap4** in $CDCl_3$; (b) the sample in (a) + **G6** (0.25 mM) in $CDCl_3$/DMSO-d_6 (96 : 4); (c) the sample in (a) + **G6** (0.50 mM) in $CDCl_3$/DMSO-d_6 (92 : 8); (d) the sample in (a) + **G6** (0.75 mM) in $CDCl_3$/DMSO-d_6 (89 : 11); (e) the sample in (a) + **G6** (1.00 mM) in $CDCl_3$/DMSO-d_6 (86 : 14); and (f) the sample in (a) + **G6** (1.25 mM) in $CDCl_3$/DMSO-d_6 (83 : 17).

the content of **G1** was increased up to 1.0 eq. (0.50 mM); in the presence of more than 1.0 eq. of **G1**, shifting occurred of the signals of **Cap4**.

Similarly, we added naphthalenetetracarboxylic anhydride (**G6**) to an equimolar mixture (0.50 mM) of **Cap2** and **Cap4** (Fig. 11 and S31†). **Cap4** bound **G6** predominantly, with the ratio of **G6@Cap4** to **G6@Cap2** being approximately five in the presence of 0.50 eq. of **G6** (0.25 mM) (Fig. 11b). When more than 2.0 eq. of **G6** (1.0 mM) was present, we could not detect any signals for free **Cap4** (Fig. 11e); in the presence of 2.5 eq. of **G6**, most of the **Cap2** dimer had recognized **G6**. During these experiments, signals for the monomeric two-armed porphyrins **P1** and **P2b** were evident, owing to the dissociation of **Cap2** in the presence of DMSO-d_6.

Although the specificity of the recognition of guests by **Cap2** and **Cap4** was not particularly high, the identities of complementary pairs of guests for **Cap2** and **Cap4** were confirmed through these competitive titration experiments.

Conclusion

We have constructed the four-armed hetero dimer capsule **Cap4** through self-assembly of a pair of porphyrin derivatives —one bearing four carboxy units at its *meso* positions and the other four 2-aminoquinolino functionalities—in CH_2Cl_2 and $CHCl_3$. The four-armed dimer capsule was kinetically and thermodynamically more stable than the corresponding two-armed dimer capsule **Cap2**. The co-facial porphyrin units of the four-armed dimer capsule **Cap4** could accommodate various electron-deficient aromatic guests; small and flexible guests were encapsulated predominantly by the two-armed dimer capsule **Cap2**, whereas the four-armed capsule **Cap4** preferred large and rigid aromatic guests. Competitive self-sorting of **Cap2** and **Cap4** occurred from a mixture of the four porphyrin components in $CHCl_3$; the two- and four-armed pairs self-assembled individually to form their corresponding hetero dimers. Furthermore, when we added **G1** and **G6** (favourable guests for **Cap2** and **Cap4**, respectively) to a mixture of **Cap2** and **Cap4**, these guest molecules were encapsulated selectively by their preferred hosts. The present results will be encourage construction of higher-order assembled multilayer π-aromatic architectures.

Experimental

Materials and methods

Compounds **1**[11] and **3**[11] and the porphyrin derivatives **P1**[11] and **P3**[18] were prepared according to literature procedures. Solvents and commercially available chemicals were used as received. ^{1}H and ^{13}C NMR spectra were recorded using JEOL ECX-500II, ECZ-500, and ECA-600II spectrometers, with tetramethylsilane as the internal standard. Mass spectra were recorded using JEOL JMS-700T (FAB), Bruker Daltonics autoflex (MALDI), and Bruker Daltonics solariX (ESI) spectrometers. Infrared spectra were recorded using a JASCO FT/IR-4100 spectrometer. All reactions were performed under a positive atmosphere of dry N_2. All solvents were evaporated

through rotary evaporation under reduced pressure. Silica gel column chromatography was performed using Kanto Chemical silica gel 60N. Thin-layer chromatography was performed using Merck Kieselgel 60PF_{254}.

Compound 2. A solution of 2-chloro-7-formylquinoline **1** (197 mg, 1.03 mmol) in neopentylamine (546 mg, 6.24 mmol) was heated at 100 °C for 10 days in a sealed tube. After cooling, THF (8.0 mL) and conc. HCl (aq) (1.0 mL) were added to the mixture. After evaporation of THF, the residue was diluted with CH_2Cl_2 and washed sequentially with H_2O, sat. Na_2CO_3 (aq), and sat. NaCl (aq). The organic phase was dried (Na_2SO_4) and concentrated. The residue was purified chromatographically (SiO_2; toluene/AcOEt, 8 : 1) to give **2** (116 mg, 47%) as a yellow solid. ^{1}H NMR (600 MHz, $CDCl_3$) δ: 1.03 (s, 9H), 3.37 (d, J = 5.5 Hz, 2H), 4.87 (br s, 1H), 6.77 (d, J = 8.9 Hz, 1H), 7.66 (d, J = 8.9 Hz, 1H), 7.69 (dd, J = 8.3, 1.4 Hz, 1H), 7.84 (d, J = 8.3 Hz, 1H), 8.12 (br s, 1H), 10.1 (s, 1H). ^{13}C NMR (150 MHz, $CDCl_3$) δ: 27.5, 32.0, 52.8, 114.0, 119.0, 127.2, 128.4, 131.6, 136.9, 137.1, 147.8, 157.9, 192.8. IR (KBr, ν_{max}, cm^{-1}): 3405, 2962, 2864, 2821, 2720, 1688, 1616, 1569, 1542, 1498, 1409, 1394, 1374, 1363, 1316, 1298, 1261, 1202, 1167, 1112, 895, 846, 742, 597, 551. HRMS (MALDI): calcd for $C_{15}H_{19}N_2O^+$ $[M + H]^+$, m/z 243.1492, found 243.1499.

Porphyrin derivative P2b. The dipyrromethane **3** (250 mg, 898 μmol) was added to a solution of the aminoquinoline **2** (282 mg, 1.16 mmol) in propionic acid (20 mL) at 130 °C and then the mixture was heated at the same temperature for 2 h and at room temperature for 2 h under air. After concentration, the residue was diluted with CH_2Cl_2, washed sequentially with sat. Na_2CO_3 (aq) and sat. NaCl (aq), dried (Na_2SO_4), and concentrated. The residue was purified chromatographically (SiO_2; toluene/MeOH, 30 : 1–20 : 1) to give **P2b** (77.6 mg, 17%) as a purple powder. ^{1}H NMR (600 MHz, $CDCl_3$) δ: −2.70 (s, 2H), 1.05 (s, 18H), 1.60 (s, 18H), 3.40 (d, J = 6.4 Hz, 4H), 4.94 (br, 2H), 6.90 (d, J = 9.6 Hz, 2H), 7.72–7.78 (m, 4H), 7.88 (d, J = 8.0 Hz, 2H), 8.07 (t, J = 8.0 Hz, 2H), 8.11–8.18 (m, 6H), 8.51–8.55 (m, 2H), 8.85 (d, J = 4.8 Hz, 4H), 8.88 (d, J = 4.8 Hz, 4H). ^{13}C NMR (150 MHz, $CDCl_3$, 25 °C) δ: 27.5, 31.7, 32.0, 34.9, 53.2, 111.6, 119.9, 120.3, 122.7, 123.6, 125.0, 129.3, 132.0, 134.5, 137.5, 139.2, 143.7, 146.6, 150.4, 158.4. Four aromatic carbon signals were missing/overlapping; broad signals were observed at 130–132 ppm at 25 °C; these broad signals became sharp at 45 °C (see Fig. S33b†). IR (KBr, ν_{max}, cm^{-1}): 3447, 3320, 2958, 2905, 2867, 1617, 1521, 1476, 1388, 1249, 1200, 1127, 969, 939, 802, 730, 629, 572. HRMS (MALDI): calcd for $C_{68}H_{71}N_8^+$ $[M + H]^+$, m/z 999.5796, found 999.5762.

Porphyrin derivative P4b. A solution of aminoquinoline **2** (366 mg, 1.51 mmol) and pyrrole (101 μL, 1.46 mmol) in propionic acid (10 mL) was heated at 140 °C for 2 h and then stirred for 11 h at room temperature under air. After concentration, CH_2Cl_2 was added to the residue and then the mixture was washed sequentially with sat. Na_2CO_3 (aq) and sat. NaCl (aq), dried (Na_2SO_4), and concentrated. The residue was purified chromatographically (SiO_2; toluene/EtOH/NEt_3, 160 : 8 : 1) to give **P4b** (75.2 mg, 18%) as a purple powder. ^{1}H NMR (600 MHz, $CDCl_3$) δ: −2.64 (s, 2H), 1.04 (s, 36H), 3.32–3.42 (m, 8H), 4.82–5.13 (m, 4H), 6.88 (d, J = 8.0 Hz, 4H), 7.83–7.91 (m, 4H), 8.01–8.14 (m, 8H), 8.50–8.57 (m, 4H), 8.87 (s, 8H). ^{13}C NMR (150 MHz, $CDCl_3$, 25 °C) δ: 27.5, 32.0, 53.2, 111.6, 120.0, 122.7, 125.0, 129.3, 132.0, 137.4, 143.6, 146.6, 158.4. Two aromatic carbon signals were missing/overlapping; broad signals were observed at 130–132 ppm at 25 °C; these broad signals became sharp at 45 °C (see Fig. S34b†). IR (KBr, ν_{max}, cm^{-1}): 3428, 3318, 2953, 2864, 1616, 1522, 1476, 1388, 1249, 1201, 1128, 974, 937, 802, 729. HRMS (MALDI): calcd for $C_{76}H_{79}N_{12}^+$ $[M + H]^+$, m/z 1159.6545, found 1159.6538.

Author contributions

M. U. synthesized and characterized compounds, and wrote the manuscript. M. K. synthesized and characterized compounds. S. M. characterized compounds. M. N. supervised the project and edited the manuscript. H. T. supervised to characterize compounds and edited the manuscript. Y. T. supervised the project and wrote the manuscript.

Conflicts of interest

There are no conflicts to declare.

Acknowledgements

FT-ICR-MS analysis was supported by the JURC at ICR, Kyoto University.

Notes and references

1 For selected reviews on porphyrin supramolecular architectures, see: (*a*) S. J. Lee and J. T. Hupp, *Coord. Chem. Rev.*, 2006, **250**, 1710–1723; (*b*) C. M. Drain, A. Varotto and I. Radivojevic, *Chem. Rev.*, 2009, **109**, 1630–1658; (*c*) I. Beletskaya, V. S. Tyurin, A. Yu. Tsivadze, R. Guilard and C. Stern, *Chem. Rev.*, 2009, **109**, 1659–1713; (*d*) S. Durot, J. Taesch and V. Heitz, *Chem. Rev.*, 2014, **114**, 8542–8578; (*e*) J. A. Wytko, R. Ruppert, C. Jeandon and J. Weiss, *Chem. Commun.*, 2018, **54**, 1550–1558; (*f*) E. G. Percástegui and V. Jancik, *Coord. Chem. Rev.*, 2020, **407**, 213165.

2 For selected examples on catalyst of porphyrin cages, see: (*a*) S. J. Lee, S.-H. Cho, K. L. Mulfort, D. M. Tiede, J. T. Hupp and S. T. Nguyen, *J. Am. Chem. Soc.*, 2008, **130**, 16828–16829; (*b*) X. Wang, S. S. Nurttila, W. I. Dzik, R. Becker, J. Rodgers and J. N. H. Reek, *Chem. – Eur. J.*, 2017, **23**, 14769–14777; (*c*) S. S. Nurttila, P. Becker, J. Hessels, S. Woutersen and J. N. H. Reek, *Chem. – Eur. J.*, 2018, **24**, 16395–16406; (*d*) C. Colomban, G. Szaloki, M. Allain, L. Gomez, S. Goeb, M. Salle, M. Costas and X. Ribas, *Chem. – Eur. J.*, 2017, **23**, 3016–3022.

3 For selected examples on changes of photophysical properties in self-assembled porphyrins, see: (*a*) K. Sugou, K. Sasaki, K. Kitajima, T. Iwaki and Y. Kuroda, *J. Am. Chem. Soc.*, 2002, **124**, 1182–1183; (*b*) Y. Kuramochi, A. Satake and Y. Kobuke, *J. Am. Chem. Soc.*, 2004, **126**, 8668–8669; (*c*) J. Aimi, Y. Nagamine, A. Tsuda, A. Muranaka, M. Uchiyama and T. Aida, *Angew. Chem., Int. Ed.*, 2008, **47**, 5153–5156; (*d*) N. Aratani, D. Kim and A. Osuka, *Acc. Chem. Res.*, 2009, **42**, 1922–1934; (*e*) C. Maeda, H. Shinokubo and A. Osuka, *Org. Lett.*, 2009, **11**, 5322–5325; (*f*) A. I. Oliva, B. Ventura, F. Wurthner, A. Camara-Campos, C. A. Hunter, P. Ballester and L. Flamigni, *Dalton Trans.*, 2009, 4023–4037; (*g*) R. F. Kelley, S. J. Lee, T. M. Wilson, Y. Nakamura, D. M. Tiede, A. Osuka, A. J. T. Hupp and M. R. Wasielewski, *J. Am. Chem. Soc.*, 2008, **130**, 4277–4284; (*h*) K. G. Dutton, D. A. Rothschild, D. B. Pastore, T. J. Emge and M. C. Lipke, *Inorg. Chem.*, 2020, **59**, 12616–12624.

4 For selected examples on other characteristic properties in self-assembled porphyrins, see: (*a*) Y. Yao, R. Zhao, Y. Shi, Y. Cai, J. Chen, S. Sun, W. Zhang and R. Tang, *Chem. Commun.*, 2018, **54**, 8068–8071; (*b*) A. K. Bar, S. Mohapatra, E. Zangrando and P. S. Mukherjee, *Chem. – Eur. J.*, 2012, **18**, 9571–9579; (*c*) H. Ube, K. Endo, H. Sato and M. Shionoya, *J. Am. Chem. Soc.*, 2019, **141**, 10384–10389; (*d*) X. Jiang, Z. Zhou, H. Yang, C. Shan, H. Yu, L. Wojtas, M. Zhang, Z. Mao, M. Wang and P. J. Stang, *Inorg. Chem.*, 2020, **59**, 7380–7388.

5 (*a*) Y. Kuroda, A. Kawashima, Y. Hayashi and H. Ogoshi, *J. Am. Chem. Soc.*, 1997, **119**, 4929–4933; (*b*) M. C. Calama, P. Timmerman and D. N. Reinhoudt, *Angew. Chem., Int. Ed.*, 2000, **39**, 755–758; (*c*) A. Ikeda, M. Ayabe, S. Shinkai, S. Sakamoto and K. Yamaguchi, *Org. Lett.*, 2000, **2**, 3707–3710; (*d*) N. P. E. Barry, M. Austeri, J. R. M. Lacour and B. Therrien, *Organometallics*, 2009, **28**, 4894–4897; (*e*) H. L. Ozores, M. Amorín and J. R. Granja, *J. Am. Chem. Soc.*, 2017, **139**, 776–784; (*f*) C. Colomban, V. Martin-Diaconescu, T. Parella, S. Goeb, C. Garcia-Simon, J. Lloret-Fillol, M. Costas and X. Ribas, *Inorg. Chem.*, 2018, **57**, 3529–3539.

6 (*a*) Y. Hatakeyama, T. Sawada, M. Kawano and M. Fujita, *Angew. Chem., Int. Ed.*, 2009, **48**, 8695–8698; (*b*) F. J. Rizzuto, J. P. Carpenter and J. R. Nitschke, *J. Am. Chem. Soc.*, 2019, **141**, 9087–9095.

7 (*a*) N. Fujita, K. Biradha, M. Fujita, S. Sakamoto and K. Yamaguchi, *Angew. Chem., Int. Ed.*, 2001, **40**, 1718–1721; (*b*) P. Ballester, A. I. Oliva, A. Costa, P. M. Deya, A. Frontera, R. M. Gomila and C. A. Hunter, *J. Am. Chem. Soc.*, 2006, **128**, 5560–5569; (*c*) Y.-R. Zheng, Z. Zhao, M. Wang, K. Ghosh, J. B. Pollock, T. R. Cook and P. J. Stang, *J. Am. Chem. Soc.*, 2010, **132**, 16873–16882; (*d*) S. K. Samanta and M. Schmittel, *Org. Biomol. Chem.*, 2013, **11**, 3108–3115.

8 (*a*) C. García-Simón, M. Garcia-Borràs, L. Gómez, I. Garcia-Bosch, S. Osuna, M. Swart, J. M. Luis, C. Rovira, M. Almeida, I. Imaz, D. Maspoch, M. Costas and X. Ribas, *Chem. – Eur. J.*, 2013, **19**, 1445–1456; (*b*) T. Nakamura, H. Ube and M. Shionoya, *Angew. Chem., Int. Ed.*, 2013, **125**, 12096–12100; (*c*) N. Ousaka, S. Yamamoto, H. Iida, T. Iwata, S. Ito, R. Souza, Y. Hijikata, S. Irle and E. Yashima, *J. Org. Chem.*, 2021, **86**, 10501–10516.

9 (*a*) T. Nakamura, H. Ube, R. Miyake and M. Shionoya, *J. Am. Chem. Soc.*, 2013, **135**, 18790–18793; (*b*) W. Meng, B. Breiner, K. Rissanen, J. D. Thoburn, J. K. Clegg and D. J. R. Nitschke, *Angew. Chem., Int. Ed.*, 2011, **50**, 3479–3483; (*c*) N. Struch, C. Bannwarth, T. K. Ronson, Y. Lorenz, B. Mienert, N. Wagner, M. Engeser, E. Bill, R. Puttreddy, K. Rissanen, J. Beck, S. Grimme, J. R. Nitschke and A. Lützen, *Angew. Chem., Int. Ed.*, 2017, **56**, 4930–4935.

10 (*a*) T. Nakamura, H. Ube, M. Shiro and M. Shionoya, *Angew. Chem., Int. Ed.*, 2013, **52**, 720–723; (*b*) F. J. Rizzuto and J. R. Nitschke, *Nat. Chem.*, 2017, **9**, 903–908.

11 M. Kimura, J. Miyashita, S. Miyagawa, T. Kawasaki, H. Takaya and Y. Tokunaga, *Asian J. Org. Chem.*, 2018, **7**, 2087–2093.

12 M. Ueda, M. Kimura, S. Miyagawa, H. Takaya, M. Naito and Y. Tokunaga, *Chem. – Asian J.*, 2020, **15**, 2212–2217.

13 We modified the side chains of amino groups in porphyrin **P4** for improvement of **Cap4** formation. This phenomenon will be reported elsewhere.

14 (*a*) Bindfit (http://supramolecular.org); (*b*) P. Thordarson, *Chem. Soc. Rev.*, 2011, **40**, 1305–1323.

15 (*a*) M. M. Safont-Sempere, G. Fernandez and F. Wurthner, *Chem. Rev.*, 2011, **111**, 5784–5814; (*b*) M. L. Saha and M. Schmittel, *Org. Biomol. Chem.*, 2012, **10**, 4651–4684; (*c*) Z. He, W. Jiang and C. A. Schalley, *Chem. Soc. Rev.*, 2015, **44**, 779–789; (*d*) H. Jedrzejewska and A. Szumna, *Chem. Rev.*, 2017, **117**, 4863–4899.

16 R. Krämer, J.-M. Lehn and A. Marquis-Rigault, *Proc. Natl. Acad. Sci. U. S. A.*, 1993, **90**, 5394–5398.

17 (*a*) K. A. Jolliffe, P. Timmerman and D. N. Reinhoudt, *Angew. Chem., Int. Ed.*, 1999, **38**, 933–937; (*b*) H. Ito, Y. Furusho, T. Hasegawa and E. Yashima, *J. Am. Chem. Soc.*, 2008, **130**, 14008–14015.

18 (*a*) J. Rochford, D. Chu, A. Hagfeldt and E. Galoppini, *J. Am. Chem. Soc.*, 2007, **129**, 4655–4665; (*b*) S. Muniappan, S. Lipstman, S. George and I. Goldberg, *Inorg. Chem.*, 2007, **46**, 5544–5554.